IKR Journal Of Engineering and Technology (IKRJET)

Journal homepage: https://ikrpublishers.com/ikrjet
Volume-1, Issue-1(March-April) 2025

ISSN:XXXX-XXXX(Online)

FEASIBILITY OF CADMIUM ADSORPTION USING *LUFFA CYLINDRICA*: MECHANISTIC INVESTIGATION OF MASS TRANSFER STAGES INVOLVED IN THE ADSORPTION PROCESS

Emene, A. U.[1*]
[1]Department of Chemical Engineering, Federal University of Technology, Minna, Niger State.

**Corresponding author: Emene, A. U.*

Abstract

Adsorption is a commonly used treatment for wastewater. The utilisation of Luffa cylindrica as an adsorbent had previously been adopted to treat wastewater laden with heavy metal ions. The investigation of Luffa cylindrica (LC), an adsorbent, applied for the uptake of the cadmium ions was carried out. The adsorption capacity was increased when the LC was treated with NaOH. The solution pH, immersion time, initial adsorbate concentration and adsorbent concentration influences the uptake of the cadmium ions. At an optimum pH range approximately within6 &8, the adsorption capacity increased. The pseudo second order kinetic and Sips isotherm models showed the best fit. The characterisation of the LC shows the presence of binding groups that aid adsorption. The mass transfer factor model (MTfM) was applied, and it showed no dependence of the metal ion adsorptive mass transfer on film diffusion. The MTfMfurther shows the impact of treated LC on the adsorption capacity. The outcome of the efficiency of LC as an excellent adsorptive material and the molecular understanding of the LC showed its potentiality to be used as an adsorbent wastewater treatment in developing countries. This material can further be utilised to produce nanomaterials to be applied in wastewater treatment.

Keywords: *Adsorption, cadmium, Luffa cylindrica (L. cylindrica), mass transfer factor model (MTfM).*

1 INTRODUCTION

Cadmium is one of the heavy metals found in amounts that exceed the WHO recommended maximum concentration requirements. This pollutant contaminates the water and land environments(Gordon, Callan, and Vickers 2008). The release of cadmium into the environment poses a major risk to health and environment, particularly in developing countries (Joseph et al. 2019). Its inhibits biological process and contaminate the environment (Mockaitis et al. 2012).

Sources of cadmium concentration found in polluted waste are anthropogenic: alloy manufacturing, battery, electroplating, mining, plastic manufacturing, smelting, fertilizers, metal refining process etc. The persistence of cadmium in the environment is as a result of exceeding its permissible limits which can cause a variety of acute and chronic disorders on ingestion (Ishfaq et al. 2013).Previous researchers have established hypertension, lung insufficiency, renal disturbances as some of the adverse effects caused by cadmium exposures. Other health problems as it relates to cadmium contamination are intestine ulceration, liver necrosis, and prostate and bronchial cancer (Mockaitis et al. 2012).This global issue requires the enforcement of adequate sustainable treatment methods for effluents.

Research carried out on the treatment of heavy metal polluted wastewater have highlighted a global need to develop low cost, environmentally friendly and effective materials to tackle this issue(3,5,6). Treatment of cadmium containing effluent has lead to the development safe alternative methods such as biosorption. Adsorption is considered a typical mass transfer process that involves the transfer of adsorbate from the bulk fluid phase to the adsorbate pores (46).

The use of biological materials with functionalised surfaces capable of removing trace metals and other contaminants from water has received much attention. These materials, are termed biosorbents, and have been used in the adsorption process during recent decades as an alternative technology(Ali, Asim, and Khan 2012). Such materials are commonly utilised for their renewable nature, and their ability to biodegrade. Current studies have focused on plant materials that are by-products of other industries, such as coconut hull, sawdust or palm kernel shells (Ali, Asim, and Khan 2012).

The loofa sponge, derived from the sub-tropical plant *Luffa cylindrica (LC),* is grown annually in Nigeria and many other countries such as China and Japan. In some countries, it is common for the loofa fruit used as a feed for poultry and as a vitamin supplement for aqua feeds. The mature fruit (fibrous residue) is used to produce sponges and gourds, and then is considered as a waste material (Ajuru and Nmom 2017). The smooth cylindrical shaped fruit is approximately 12cm long, the reticulate matrix which consists of various fibrous interwoven cords are found in the sponge-like flesh material.The cords are made up of parenchyma cells, which areresponsible for the plant metabolic activities. This makes up the cellular structure. The cords comprises cylindrical fibres which are flexible and hollow(10,11) and are composed of fibrils. Resinous lignocellulose material comprising of 55-90% cellulose, 10-23% lignin, 8-22% hemicellulose make up the fibrils and the exact percentage depends on the plant origin, weather conditions, nature of soil, etc. This lignocellulosic material make up the inner part of the loofa fruit which forms the typical loofa sponge used in this research and its dried form has been used as a domestic cleaning material for years (Emene and Edyvean 2019).

The *LC* has a large proportion of cellulose material, which is used to remove heavy metal ions from aqueous solution. Studies have reported the *LC* material to possess the ability to remove both metal cations (Emene and Edyvean 2019) and organic pollutants from aqueous solutions due to the presence of active functional groups within the molecular structure(Dubey, A.Shiwani 2012). Suhas *et al.* (Suhas et al. 2016), modified cellulose, present in *LC*, by chemicals to improve the heavy metal adsorption capacity. This enhancement attributes to an increased surface area and easily accessible functional groups for further adsorption (Suhas et al. 2016).

LC represents a low cost, renewable, biodegradable solution for sustainable water treatment plants in developing countries (I. O. Oboh and Aluyor 2009). To successfully develop this as a sustainable process on a large scale, it is important to understand the surface properties of *LC*, the metal speciation of the cadmium ions removed from water, chemistry of adsorption and wastewater streamsin order to optimize the process.

This paper will investigate the efficiency process of chemically treated *LC* as an adsorbent in the removal of cadmium ions from aqueous solution, across the pH range 3-9. The adsorptive mass transfer resistance was explained during the adsorption of cadmium via the mass transfer model. The simple methodology used for the modification of the *LC* and results obtained contribute to a further understanding of the relationship between cadmium ion adsorption and *LC* properties (*LC*-Cd adsorption mechanism) under optimum conditions which attributes to a promising optimization wastewater treatment strategy for developing countries.

2 Material and methods

2.1 Reagents and stock solutions

The chemicals used were of analytical grade. The stock solution of 1 g/L of Cd (II) was prepared by dissolving cadmium sulfatesalt, obtained from Sigma-Aldrich, United Kingdom, in deionised water. The desired concentrations were obtained by diluting the stock solution at a varied concentration from 50 to 200mg/L. 0.1 M HCl and NaOH solutions were used to alter the solution pH.

2.2 Chemical Modification of Luffa Cylindrica (LC)

This is the surface clean up and preparation process for the treatment of LC(Akhtar, Iqbal, and Iqbal 2003). The LC (dried fibres) was purchased in the United Kingdom. The surface impurities and seeds were removed by washing with distilled water, then alkali treated by soaking in 4% NaOH at room temperature for 1h. The LC fibres were washed in distilled water until the pH was almost neutral, and then dried in the oven at a temperature of 90 °C for 24h.The samples were then ground and sieved to a 1 mm particle size fraction. The dried samples were stored for utilization in further experiments.

2.3 Characterisation of chemically treated LC (ATLC)

2.3.1 Surface Analysis of chemically treated LC and LC

The surface of the loofa was analysed by an Analytical Scanning Electron Microscope (SEM) (Model JOEL JSM-6010LA) coupled with energy dispersive X-ray (EDX) with an accelerating voltage of 10kV and at a magnification of x550 SS60.The chemical characteristics was analysed by using a Nicolet 6700 Fourier Transform Infra-red (FT-IR) Spectrometer to identify the functional groups that interact with cadmium ions.50mg of ATL Csample (< 250µm thickness) were prepared for ATR- FTIR analysis. Measurements were made in transmittance mode using a spectral resolution of $4cm^{-1}$ by 256 scans and approximately 150 seconds per step across the range $4000cm^{-1}$ to 650 cm^{-}

[1].The surface area of each sample of ATLC was determined from nitrogen adsorption at 77.2K in the range of relative pressure (p/p^0) of 0.05 – 1 by using a Micromeritics 3Flex instrument. The samples were degassed at 150°C for 24 hours. A three-parameter non-linear fitting procedure was utilised and the ATLC samples were subjected to a 99-point BET surface analysis. Adsorption isotherms were produced for the ATLC samples. The conventional single point method of relative pressure was used.

2.4 Batch adsorption experiments

All batch studies were performed as single contacts with the contact of 1g of 1mm size of ATLC with 200 mL of cadmium ion aqueous solution. Experiments were done at concentration range of 50 to 200mg/L; and at pH each of 3, 5, 7 and 9. High concentrations were used to determine the relationship during adsorption because lower concentration showed a high adsorption capacity that could not show an entire mass transfer mechanism for this research. The ATLC and aqueous solution were mixed for 24 hrs at an agitation speed of 200rpm at 21 °C on a magnetic stirrer. The adsorption behaviour was determined using the following;

$$q_e = \left(\frac{C_i - C_e}{C_e}\right) \times \frac{v}{m} \quad (1)$$

q_e is the weighted distribution of the metal ions where C_i is the initial aqueous concentration of the cadmium ions before contact and C_e is the aqueous concentration of the cadmium ions after equilibration. V is the volume of the aqueous phase (mL) and m is the mass of the ATLC (g). The percentage removal (R%) was determined by difference (using eqn. 2) and the concentrations of the cadmium determined by ICP-MS.

$$R\% = \frac{C_i - C_e}{C_i} \times 100 \quad (2)$$

Where C_i is the initial metal concentration before contact and C_e is the concentration of the cadmium ion in the aqueous solution after contact with the ATLC. pH measurements for solutions were determined using a silver/silver chloride reference electrode calibrated from pH 4-7 using buffers. The error was determined using the aqueous solution concentrations prior to contact (triple measurements).

2.5 Determination of adsorption isotherm behaviour

All adsorption isotherms were carried out as single contacts with the contact of 1 g of *ATLC* with 200 mL of aqueous solution. Commonly used two parameter fitting model, was used to determine the fitting ability due to its quantitative criteria for evaluation(17,18). The 3 parameter model which gives a clearer evaluation of the data was also utilised. The data were fitted to Langmuir, two site Langmuir (Vilar et al. 2009), Temkin and Sips models, equations (3-8).

2.6 Calculations

The fitting was carried out by using linear regression and by non-linear least squares analysis using Graph Pad (Vilar et al. 2009).

Langmuir

$$q_e = \frac{K_L C_e}{1 + a_L C_e} \quad (3)$$

The monolayer saturation capacity, q_m (mg L^{-1}), was calculated from the Langmuir equation using equation (4).

$$K_L = q_m a_L \quad (4)$$

Two site Langmuir

$$q_e = \frac{Q_1 b_1 C_e}{1 + b_1 C_e} + \frac{Q_2 b_2 C_e}{1 + b_2 C_e} \quad (5)$$

Temkin

$$q_e = \frac{RT}{b_T} ln(A_T C_e) \quad (6)$$

Sips

$$q_e = \frac{K_s C_e^{\beta s}}{1 + a_s C_e^{\beta s}} \quad (7)$$

Error measurements in the isotherm constants was calculated from the linear form of the model using the calculated values obtained from Excel via deviations of the experimental data from the best fit line.

2.7 Determination of the kinetics of extraction

The kinetics was carried out with the contact of 1 g of *ATLC* with 200 mL of aqueous phase. The *ATLC* and aqueous solution were mixed for a period of 24 hrs at room temperature and 5 mL samples were collected at set time intervals. The data was fitted using a linear fit of pseudo second order models, but do not take into account the mechanism of reaction.

The linear form of the pseudo-second-order kinetic model (Foo and Hameed 2010) is as follows;

$$\frac{t}{q_t} = \frac{1}{k_2 {q_e}^2} + \frac{1}{q_e} t \quad (8)$$

Where k_2 = pseudo second order reaction constant (hr^{-1}). The non-linear form for the pseudo second-order kinetics is given below;

$$q_t = \frac{k_2 q_e^2 t}{1 + k_2 q_e t} \quad (9)$$

The non-linear form was fitted using the minimization of the sum of square errors (SSE) using SOLVER(Yang et al. 2014). The $t_{1/2}$ was calculated by the relationship;

$$t_{1/2} = \frac{1}{k_2 q_e} \quad (10)$$

The initial sorption rate h_0(Foo and Hameed 2010) is given by;

$$h_0 = k {q_e}^2 \quad (11)$$

Film and pore diffusion

$$t_{1/2} = 0.03 \frac{r_o^2}{D_p} \quad (12)$$

Where Dp is the pore diffusion coefficient

$$t_{1/2} = 0.23 \frac{r_o \partial}{D_f} \times \frac{\dot{c}}{c} \quad (13)$$

where Df is the film diffusion coefficient.

The equation (12) was used to calculate the pore and film diffusion coefficient to determine the rate-controlling step of the sorption process.

The Boyd model confirms the external mass transfer as the rate-limiting step of the sorption process.

Boyd model

$$Bt = -0.4977 - In(1 - F) \quad (14)$$

A simplification of the mass transfer model is presented in equation (15) and equation (16):

$$= In\, q_e = B + \frac{1}{\beta} \times In\, t \quad (15)$$

Where B and $\frac{1}{\beta}$are the intercept and slope respectively. $B = In\,([K_L{}^a]g) - In\{In\left(\frac{C_o}{C_e}\right)\}/\,\beta$ (16)

Where $[K_L{}^a]_g$ gives the global mass transfer factor.

3 Results and Discussion

3.1 Chemical modification of Luffa cylindrica (LC)

The morphology observation of LC, shown in Figure 1, appears flaky dry with a large amount of single particles on the surface. In Figure 2, the morphology of the ATLC is broken up with a less number of loose particles on the surface. This may be as a result of the removal of the lignin and hemicellulose compounds and exposed pores (Nong, Zhou, and Wang 2016).Ghali et al. (Ghali et al. 2009)showed that to treatL. cylindrica fibres with 4 % NaOH gives it a higher crystallinity index and improves its adhesion behaviour(Ghali et al. 2009).

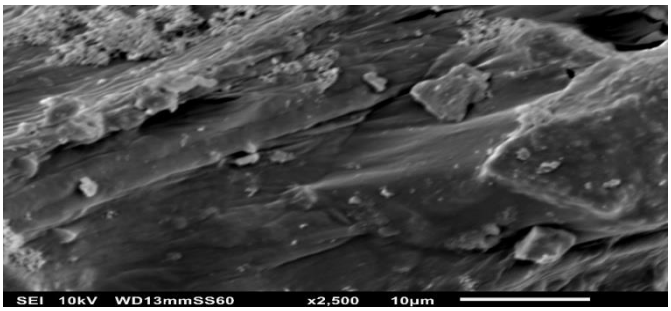

Figure 1: Surface morphology of untreated loofa (raw loofa)

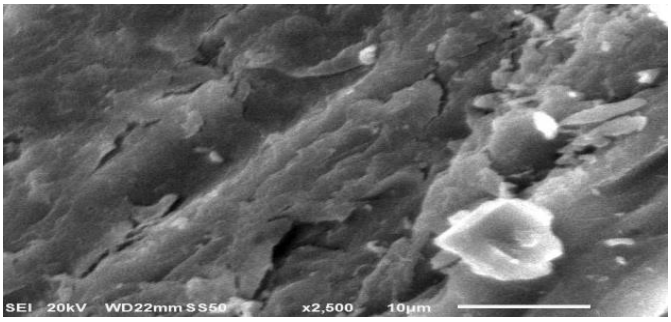

Figure 2: Surface morphology of *ATLC*

The surface properties of *ATLC* was enhanced after treatment with alkali. 4% NaOH was successfully used without damage to the crystalline region of the LC because researchers have reported the maximum percentage of NaOH to treat *L. cylindrical* to be at 8%. Ghali *et al.*(Ghali et al. 2009), investigated the pre-treatment of Luffa fibres by 4% NaOH that led to successful delignification(Ghali et al. 2009). This modification displays additional functional groups of OH^- have been added onto the surface area of *L. cylindrica* (22,23).

The surface characteristics of the *ATLC* with a BET surface area of 43.10m^2/gis higher than the untreated *LC* at 25.32m^2 /g (Table 1). This shows an increased surface area. This increase in surface area and pore volume after alkali treatment by 41.3% and 29.4% respectively shows the involvement of the *LC* surface and pore particles in improving the adsorption process.

Table 1. BET result values of the chemically treated*(ATLC)* and untreated *L. cylindrica (LC)*

Data	Untreated	4% NaOH treated
Surface area	25.32m^2/g	43.10m^2/g
Specific surface area	5.75m^2	7.00m^2
Total pore volume	0.012cm^3/g	0.017cm^3/g

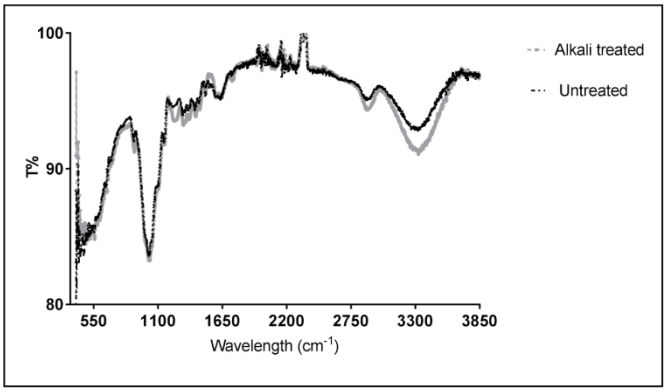

Figure 3: FT-IR spectra of *ATLC* and untreated loofa at 21°C, 256 scans

Figure 3& 4 show the changes in the bands surface chemistry during adsorption with the untreated and treated *LC*. These show characteristic functional groups on the *LC* across the 800cm^{-1} to 4000cm^{-1}range, The peak at 3340 cm^{-1} is attributed to the stretching vibration of the O-H group. A shift to 3323cm^{-1} and 1040cm^{-1} shows a change in the binding energy pattern(10,17,22). The stretching vibration at band range 1035cm^{-1} and 1250cm^{-1} are attributed to the cellulose while the characteristic bands at 1450cm^{-1} to 1600$cm^{-1}$are attributed to lignin. The peak at 1735cm^{-1} and 1550cm^{-1} changes which shows the disappearance of hemicellulose and lignin(Rodriguez Correa, Otto, and Kruse 2017).The main adsorption bands are shown to have changed (various functional groups)in Table 2. This change depicts the effect of alkali treatment. The presence of O-H groups

(exchangeable protons) are attributed to a higher and stronger band at 3100cm^{-1} to 3600cm^{-1}. This stronger band exposes the hydroxyl groups for adsorption(25,26). The stretching band in range 3545 to 3050cm^{-1} indicates characteristic strong intramolecular hydrogen bonds that leads to strong adhesion adsorption properties(27,28).

Table 2: Change in transmission FTIR results at specific regions of absorbance

Region	ΔT%	Corresponding absorbance	Reference
1265cm^{-1}-1460cm^{-1} (fingerprint region)	+0.6 - +1.1	O-H bending	(29,30)
1540cm^{-1}	-0.85	N-H bending	(Anastopoulos, Massas, and Ehaliotis 2013)
1735cm^{-1}	+0.6	C=O stretching (carbonyl group of ketone)	(Jayamani et al. 2014)
2890cm^{-1}	+0.8	C-H stretching	(10,20)
3340cm^{-1}	+1.6	O-H bonding	(10,16,29)

Alkali treatment disrupts the hydrogen bonding of OH^- functional groups on the *LC* thereby removing off H^+ for adsorption of ions(23,32). Carboxyl group are the dominant functional groups of *ATLC* in adsorption. Therefore, the difference in the binding energy of the functional groups as shown by the spectra peaks in Figure 3 indicates the importance role of O-H in the adsorption of cadmium ions onto *ATLC*. The *LC* possesses lignin, cellulose and hemicellulose and this is shown by the presence of the characteristic bands, which shows the functional groups on the *LC* surface (Emene and Edyvean 2019).Figure 4 shows an increase in the zeta potential values and when treated with alkali depicts an increase towards linearity. The *LC* structure changes after modification with alkali. This is compared to the untreated cucumber peel, a biological material that contains cellulose, hemicellulose and lignin, and possesses carboxyl and hydroxyl groups. This material shows a negatively charged surface that increases in the zeta potential values as the pH is increased from pH 2 to 6 (Saueprasearsit, Nuanjaraen, and Chinlapa 2010). Lower pH tends to cause the colloids in the system to coagulate and form more particles that are visible in solution. The zeta potentials of *ATLC* over the pH range of 2 – 10 shows a negative surface charge on the *LC* (Emene and Edyvean 2019). The increase in the magnitude of the negative zeta potential of *ATLC* in solution shows the availability of free functional groups available for exchangeable protons in adsorption which creates bonds on the surface and these protons are responsible for the charge created on the *LC* surface (Emene and Edyvean 2019). The zeta potential increases as pH increases, which suggest a potential stability for cadmium adsorption as pH increases. The negative surface charge at increased pH 6 to 8, shows the increased zeta potential. This further explains the various factors that contribute to the adsorption mechanism of cadmium ions onto *LC*. Since formation of hydroxylated cadmium ions are expected over pH 6 (shown in figure 7), pH 5 -7 (optimum mV values) is determined as the appropriate pH for an effective adsorption process (Emene, 2018).

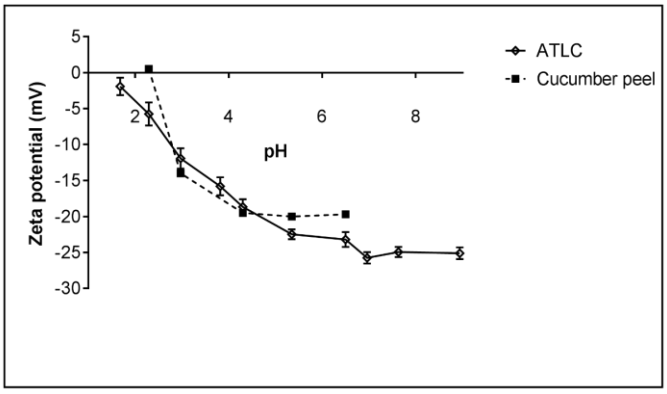

Figure 4: The zeta potential of *ATLC* and cucumber peel at constant ionic strength in aqueous solution as a function of pH

As compared to the chitin-lignin material which possesses a high carbon content and the grafted *LC* sponge, the presence of a negative zeta potential value over a range of pH 1 to 12 is attributed to the presence of specific functional groups, such as -COOH and -OH, which facilitate the adsorption process of cadmium ions(34,35).

3.2 Adsorption studies as a function of acid and anion concentration onto ATLC.

The effect of pH on the adsorption of cadmium onto *ATLC* is shown in Figure 5. It can be seen that the percentage removal shows a maximum uptake at pH 7.

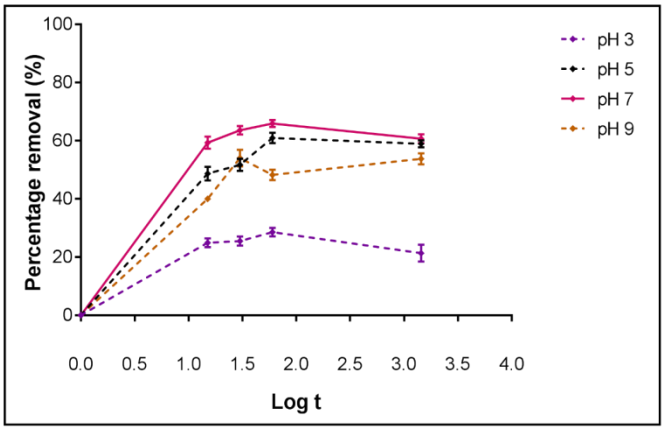

Figure 5: Effect of solution pH conditions on the percentage removal of Cd after 24hrs contact; cadmium ion concentration: 50mg/L; agitation speed: 200rpm; at temperature 21ºC, 5g/l biosorbent dosage

pH is the most important controlling factor in the adsorption process of heavy metal ions (Saeed et al. 2009). There is the competition of H^+ ions for the binding sites on *ATLC* when the equilibrium pH is below 5 thereby decreasing the adsorption capacity. This lowers the adsorption process. At pHs greater than 6 the reduced in removal of cadmium ions is most likely attributed to the hydrolysis of the cadmium ion in aqueous solutions. This depicts the difference in cadmium species and their ability to be adsorbed at different solution pH. The optimum adsorption of cadmium ions occurs below the point of zero charge (pH_{pzc} of 7.2).It is observed above pH 6 to be stable and this shows an initial maximum adsorption (Figure 6). Therefore, the results show the dominance of the adsorption process to be attributed to exchangeable ions present and other adsorption mechanisms involved (Iqbal et al. 2009).As shown in Figure 6, the cadmium species present ($Cd(OH)_2$) at pH 6 and above gives approximately 50% of the cadmium available for adsorption. The potential effect of the cadmium ion speciation as a function of pH is presented in Figure 6 and carried out using Hyss2009 program and stability constants from the NIST database.The protonated complexes $Cd(OH)_4^{2-}$build up to a maximum of below 20% of hydroxylated Cd as it relates to free Cd ions. The attachment of cadmium ions onto the surface of *LC* occurred at above pH of 6 and this shows that Cd $(OH)_2$ are being attached during the adsorption process. Furthermore, above pH 6, hydroxylated forms of the cadmium ionsare expected to precipitate which leads to a reduced adsorption capacity. The loss of cadmium ions from solution cannot be ascertained to be all due to adsorption onto the *LC* surface. At pH 4.8, free cadmium ions are disappearing as the $Cd(OH)_2$ start to formas the pH increases. The cadmium ions, $Cd(OH)_2$dominant form), complexes are formed with the dominant active charged sites on the *LC* surface. The percentage values for optimum adsorption of cadmium at optimum pH values were reported in literature (38,39).

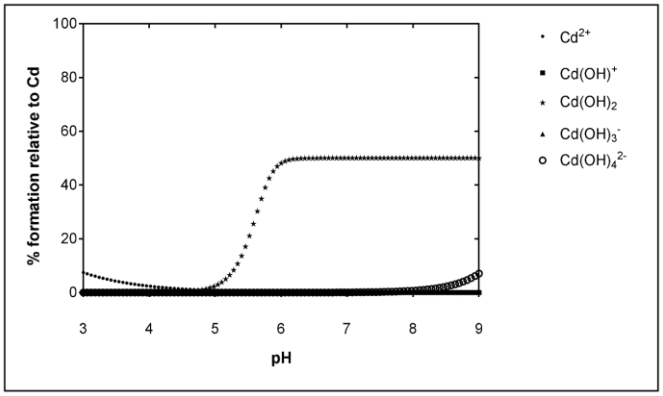

Figure 6: Distribution of cadmium nitrate species in aqueous solution at 21^0C as a function of pH (Ekberg and Brown 2016).

3.3 Isotherm behaviour of removal

The isotherm fitting parameters for all the isotherm models tested is given in Table 3 based on linear regression and non-linear regression using Graph Pad(20,63). The isotherms are used to determine the best fit in order to explain and suggest the model that best predicts the adsorption process that occurs(I. Oboh, Aluyor, and Audu 2009). The isotherm fitting parameter was calculated using various models as shown in equations 3- 7 for cadmium adsorption onto *ATLC* at 21 °C for a contact time of 24 hrs. This was done by utilising the non-linear least squares fitting using Graph Pad and SOLVER. The equilibrium concentration and adsorption capacity relationship is depicted in Figure 7.

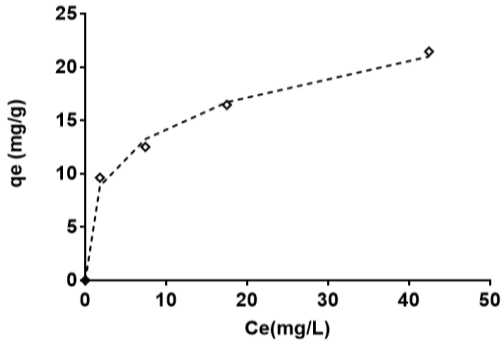

Figure 7: Cadmium isotherm from pH 7.0 ± 0.1 at 21 °C and 24 hr. contact time. Sips model fit shown by dashed line

None of the utilised isotherm models, two site Langmuir, Langmuir and Temkin satisfactorily predicted the experimental data but all fitted to a R^2 value over 0.9. The adsorption behaviour of cadmium ions fitted the Sips model and was shown (Figure 7) to give the best fit with a R^2 value of 0.928. The model fittings to the Sips model did not show a heterogeneous adsorption on the *LC* surface, which possesses both weak and strong sites but a monolayer homogeneous surface adsorption. The activation energy, which shows a chemisorption mechanism that involves both the surface and pores of the *LC* is as a result of the presence of two different sites which are available for adsorption.Furthermore, it explains and supports the different mechanisms of the adsorption process that occur with the utilisation of *LC* and explicitly explains the mechanism process.

The adsorption capacity of cadmium ions are enhanced by modification with alkali treatment. Optimum removal of cadmium ions ($Cd(OH)_2$) is at pH 7 with a 60.7% percentage removal and the loss of cadmium ions from solution cannot be ascertained to be attributed to adsorption onto the *LC* surface because of the precipitated hydroxylated forms of cadmium. Compared to other adsorbents, such as 55% of cadmium adsorption by polyphosphate-modified kaolinite clay (Amer, Khalili, and Awwad 2010), the modified loofa (*ATLC*) shows a greater percentage removal of cadmium ionsat 21^0C.

3.4 Kinetics of extraction

The batch kinetic models are adequately utilised because they are essential in the explicit description of the adsorption

mechanism and to determine the potential controlling steps of mass transfer. The obtained results shows a best fit to the pseudo-second order (PSO) (Figure 9)(Graph Pad Prism)which shows the involvement of two species in the sorption process of cadmium ions. As agreed with literature, a pseudo second order model best describes the adsorption of divalent metal ions(Vilar et al. 2009). The rate constant of a pseudo second order model (k_2) rises and falls as pH is increased (Table 5).And (k_2) increases as concentration increase still a peak is reached (Table 6). This depicts a reduced adsorption rate and the resistance in the micropores is increased, till the peak is at equilibrium(Emene 2015). The PSO model fit has a R^2 value of above 0.9 for each utilised concentration and pH as shown in Table 5 and 6. The fastest exchange rate occurred between 2 and 15mins and this may further be explained that the exchange positions are initially on the surface**.** The increase in initial concentration leads to in an increase in K_2 and then a decrease. Further decrease in K_2showed further increase in concentration. This implies that a faster adsorption occurs at lowest concentration because it shows the lowest k_2 value. Other experimental factors imply that diffusion and other factors play an important role in the kinetic process of adsorption of cadmium ions. This kinetic process explicitly explains the relationship between the number of available adsorption sites and the rate of adsorption. The availability of binding sites relates to the initial concentration of cadmium ions and the equilibrium time once adsorption capacity is occurs(45,46). The change in the k_2 value when concentration increased is explained due to a decrease in the adsorbates' chemical potential which limits their driving force (Mohamed et al. 2021).

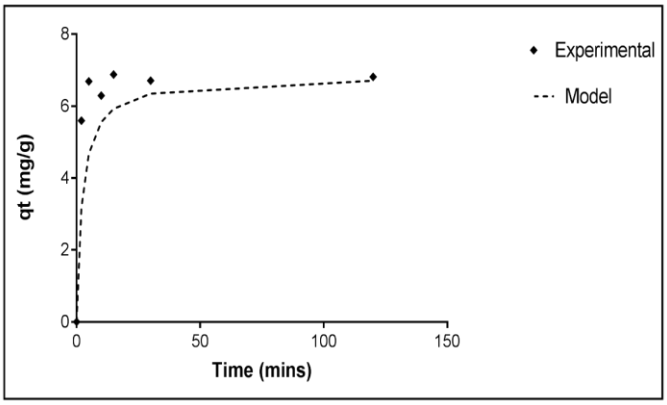

Figure 8: Pseudo second order kinetic using non-linear regression in SOLVER (Hossain, Ngo, and Guo 2013), ◆= 50mg/L, Cd^{2+} in solution at pH 7.0 ± 0.1 at 21 °C.PSO model shown with dashed line

Model efficiency, which equates to the correlation coefficient R^2 value, is a good measure to avoid errors that may occur due to the experimental data values and it is the best indicator for model fitting data values. The non-linear chi square test values also confirm the best fit of the model to the experiment data of the adsorption process system. More accurate estimations are implied with smaller NSD values(47,48).

3.5 Mechanistic mass transfer model:

It represents the plot of Inqe versus In t which gives a straight line.

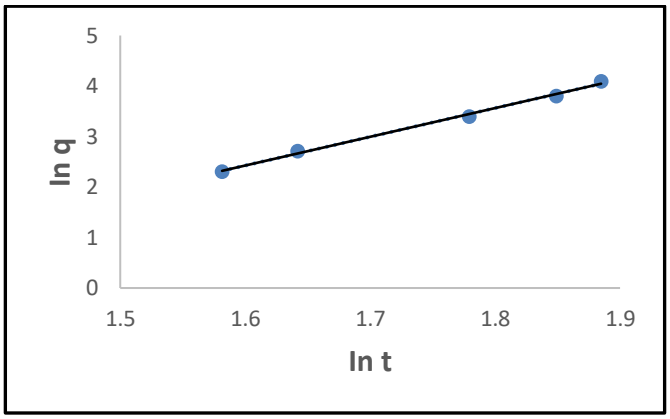

Figure 9: Linear regression for cadmium adsorption from pH 7.0 ± 0.1 at 21 °C and 24 hr. contact time. Mass transfer model fit shown by line

The plot of Inq_e versus Int (Figure 10) shows a good correlation with an R^2 value of 0.997. The intercept (B (mg/g) and slope (1/β (g h/mg) values, 5.69 and -6.68 respectively, explains the definition of the mass transfer potential and the adsorbate-adsorbent affinity as it relates to the cadmium adsorption mechanism. The negative B value is attributed to decline in the adsorption driving force as the cadmium ion concentration in the bulk fluid reduces. The presence of a low mass transfer factor explains the presence of a significant affinity between *LC* and cadmium ions during the adsorption process (Mohamed et al. 2021).PSO k_2 values at a higher and lower concentration, shows that sorption and desorption occur as the cadmium ions concentration increased in value. This shows that film diffusion is the controlling step in the mass transfer process and it is not predominantly represented as the concentration increases. This means at a lower concentration the adsorption system is not explained by film diffusion.

Table 3: Kinetic parameters of pseudo second order (Linear regression) at varying pH values at 21 °C

pH	q_e (mg·g^{-1})	h_0 (mins)	k_2 (g·mg^{-1}·min^{-1})	R^2
3	3.032	1.73E-01	0.078	0.997
5	6.743	9.43E-01	0.021	0.994
7	6.840	2.96E-00	0.063	1.000

Table 4: Kinetic parameters of pseudo second order (Linear regression) at pH 7 at 21 °C

Concentration (mg/L)	q_e ($mg \cdot g^{-1}$)	R^2	k_2 ($g \cdot mg^{-1} \cdot min^{-1}$)
50	5.672	0.985	0.012
70	5.896	0.990	0.013
100	6.845	0.999	1.906
150	8.292	0.994	0.225

4 Conclusions

This report results show that *LC* has a promising potential in the removal of cadmium ions from aqueous solutions. The NaOH treatment of *LC* improves the adsorption capacity. The results from the negative zeta potential show a negatively charged *LC* surface. The change in frequency obtained from the characteristic bands due to vibrations at prominent peaks on the *LC*, shows the functional groups involved in the adsorption process onto the *LC*. The uptake efficiency of Cd (II) indicates dependence on pH, cadmium ion concentration and time. The optimum pH of the adsorption of cadmium ions by *LC* at 21ºC was at pH 7 at equilibrium. The Sips isotherm model showed the best fit. The removal of Cd (II) ions is negatively affected by the possible desorption of the hydroxylated forms of cadmium ions present in the aqueous solution. The kinetics model fit indicated that the PSO model gives the best fit and the adsorption rate was at 0.225g/mg/min at150mg/L. The mass transfer factor gives insight into the mass transfer resistance, therefore the sorption processes of the cadmium ions by loofa were not solely controlled by film diffusion mechanism. This shows a feasible chemisorption reaction.

Cadmium ion adsorption as compared to few researchers have been found to have a higher maximum loading capacity than *LC* used in this report but because the *LC* material is economically viable, widely available in Nigeria, does not require a surface properties' modification process that is expensive, it utilises no extensive technological applications and can also easily accessible in large quantities, it is regarded as a sustainable material on a global scale(49,50).

Loofa is easily grown in large quantities and its accessibility can support in it being widely used in developing countries. The design of this adsorption system and potential nanotechnology with *LC*, as the biosorbent, will help to create internal revenue in Nigeria and also assist in tackling the environmental issues in the Niger Delta and other parts of the country(9,50).

Conflict of interest

The author declare no conflict of financial interests.

Acknowledgement

This research was funded by a grant from the Nigerian government for scholarship funding (Niger Delta Development Commission (NDDC)/DEHSS award). All ICP-MS analysis was carried out by Kroto Research Institute, Groundwater Protection and Restoration Group (KRIGPRG), The University of Sheffield. Thanks to KRIGPRG staff. FT-IR analysis was carried out at Kroto Research Institute, The University of Sheffield. Thanks to Dr. Robert Edyvean. Thanks to the Department of Chemical and Biological Engineering of The University of Sheffield.

5 References

1. Agbabiaka, L. A., K C Okorie, and C F Ezeafulukwe. 2013. "Plantain Peels as Dietary Supplement in Practical Diets for African Catfish (Clarias Gariepinus Burchell 1822) Fingerlings . Department of Fisheries / Marine Technology , Imo State Polytechnic , Umuagwo , Nigeria," 155–59. doi:10.5251/abjna.2013.4.2.155.159.
2. Ajuru, Mercy, and Felicia Nmom. 2017. "A Review on the Economic Uses of Species of Cucurbitaceae and Their Sustainability in Nigeria." *American Journal of Plant Biology* 2 (1): 17–24. doi:10.11648/J.AJPB.20170201.14.
3. Akhtar, Nasreen, J Iqbal, and M Iqbal. 2003. "Microalgal-Luffa Sponge Immobilized Disc: A New Efficient Biosorbent for the Removal of Ni(II) from Aqueous Solution." *Letters in Applied Microbiology* 37 (Ii): 149–53.
4. Ali, Imran, Mohd Asim, and Tabrez a. Khan. 2012. "Low Cost Adsorbents for the Removal of Organic Pollutants from Wastewater." *Journal of Environmental Management* 113 (December). Elsevier Ltd: 170–83. doi:10.1016/j.jenvman.2012.08.028.
5. Amer, Mohammad W, Fawwaz I Khalili, and Akl M Awwad. 2010. "Adsorption of Lead , Zinc and Cadmium Ions on Polyphosphate-Modified Kaolinite Clay" 2 (1): 1–8.
6. Anastopoulos, I., I. Massas, and C. Ehaliotis. 2013. "Composting Improves Biosorption of Pb2+and Ni2+ by Renewable Lignocellulosic Materials. Characteristics and Mechanisms Involved." *Chemical Engineering Journal* 231. Elsevier B.V.: 245–54. doi:10.1016/j.cej.2013.07.028.
7. Arshadi, M, M J Amiri, and S Mousavi. 2014. "Kinetic, Equilibrium and Thermodynamic Investigations of Ni(II), Cd(II), Cu(II) and Co(II) Adsorption on Barley Straw Ash." *Water Resources and Industry* 6: 1–17. doi:http://dx.doi.org/10.1016/j.wri.2014.06.001.
8. Bai, R Sudha, and T Emilia Abraham. 2002. "Studies on Enhancement of Cr(VI) Biosorption by Chemically Modified Biomass of Rhizopus Nigricans." *Water Research* 36 (5): 1224–36. doi:http://dx.doi.org/10.1016/S0043-1354(01)00330-

X.
9. Benhima, H, M Chiban, F Sinan, P Seta, and M Persin. 2008. “Removal of Lead and Cadmium Ions from Aqueous Solution by Adsorption onto Micro-Particles of Dry Plants.” *Colloids and Surfaces. B, Biointerfaces* 61 (1): 10–16. doi:10.1016/j.colsurfb.2007.06.024.
10. Boudechiche, N, H Mokaddem, Z Sadaoui, and M Trari. 2016. “Biosorption of Cationic Dye from Aqueous Soutions onto Lignocellulosic Biomass (Luffa Cylindrica): Charcaterisation, Equilibrium, Kinetic and Thermodynamic Studies.” *International Journal of Industrial Chemistry* 7 (2): 167–80. doi:10.1007/s40090-015-0066-4.
11. Dubey, A.Shiwani, S. 2012. “Adsorption of Lead Using a New Green Material Obtained from Portulaca Plant.” *International Journal of Environental Science and Technology* 9: 15–20. doi:10.1007/s13762-011-0012-8.
12. Ekberg, C., and P. L. Brown. 2016. “Hydrolysis of Metal Ions,” 675–835. doi:10.1002/9783527656189.
13. ElShafei, Gamal M.S. S, Ibrahim M.a. A ElSherbiny, Atef S. Darwish, and Christine a. Philip. 2014. “Silkworms’ Feces-Based Activated Carbons as Cheap Adsorbents for Removal of Cadmium and Methylene Blue from Aqueous Solutions.” *Chemical Engineering Research and Design* 92 (3). Institution of Chemical Engineers: 461–70. doi:10.1016/j.cherd.2013.09.004.
14. Emene, Akanimo. 2015. “Biosorption of Certain Selected Toxic Heavy Metals and Methylene Blue by Use of Anionised Chlorella Kesslerii and Phanerocheate Chrysosporium Loaded Luffa Cylindrica.”
15. ———. 2018. “The University of Sheffield Biosorption of Selected Heavy Metal Ions and Methylene Blue from Aqueous Solution Using Chemically Treated.”
16. Emene, Akanimo, and Robert Edyvean. 2019. “Removal of Pb(II) Ions from Solution Using Chemically Modified Luffa Cylindrica as a Method of Sustainable Water Treatment.” *International Journal of Scientific & Engineering Research* 10 (2): 344–64. doi:10.1016/B978-0-444-42615-4.50012-6.
17. Foo, K.Y. Y, and B.H. H Hameed. 2010. “Insights into the Modeling of Adsorption Isotherm Systems.” *Chemical Engineering Journal* 156 (1): 2–10. doi:10.1016/j.cej.2009.09.013.
18. Ghali, L., S. Msahli, M. Zidi, and F. Sakli. 2009. “Effect of Pre-Treatment of Luffa Fibres on the Structural Properties.” *Materials Letters* 63 (1). Elsevier B.V.: 61–63. doi:10.1016/j.matlet.2008.09.008.
19. Gordon, B., P. Callan, and C. Vickers. 2008. “WHO Guidelines for Drinking-Water Quality.” *WHO Chronicle* 38 (3): 564. doi:10.1016/S1462-0758(00)00006-6.
20. Hassan, M. 2006. “Quaternization and Anion Exchange Capacity of Sponge Gourd (Luffa Cylindrica).” *Applied Polymer* 101 (4): 2495–2503. doi:10.1002/app.23747.
21. Hossain, M A, Huu Hao Ngo, and Wenshan Guo. 2013. “Introductory of Microsoft Excel SOLVER Function - Spreadsheet Method for Isotherm and Kinetics Modelling of Metals Biosorption in Water and Wastewater.” *Journal of Water Sustainability* 3 (4): 223–37.
22. Iqbal, Muhammad, Asma Saeed, Saeed Iqbal Zafar, and Saeed Iqbal. 2009. “FTIR Spectrophotometry, Kinetics and Adsorption Isotherms Modeling, Ion Exchange, and EDX Analysis for Understanding the Mechanism of Cd2+ and Pb2+ Removal by Mango Peel Waste.” *Journal of Hazardous Materials* 164 (1): 161–71. doi:http://dx.doi.org/10.1016/j.jhazmat.2008.07.141.
23. Ishfaq, Tahir, Sajida Naveed, Mohsin Kazmi, H A Q Nawaz, and Nadeem Feroze. 2013. “A DETAILED INVESTIGATION ON ENGINEERING PARAMETERS FOR Cd (II) REMOVAL BY RIPPED CITRUS PARADISI PULP WASTE” 4: 2–6.
24. Jayamani, E., S. Hamdan, S. K. Heng, M. R. Rahman, M. K. Bakri, and A. Kakar. 2014. “The Effect of Natural Fibres Mercerization on Natural Fibres/Polypropylene Composites: A Study of Thermal Stability, Morphology and Infrared Spectrum.” *Australian Journal of Basic and Applied Sciences* 8 (1991–8178): 332–40.
25. Joseph, Lesley, Byung Moon Jun, Joseph R.V. Flora, Chang Min Park, and Yeomin Yoon. 2019. “Removal of Heavy Metals from Water Sources in the Developing World Using Low-Cost Materials: A Review.” *Chemosphere*. doi:10.1016/j.chemosphere.2019.04.198.
26. Lasheen, Mohamed R., Nabila S. Ammar, and Hanan S. Ibrahim. 2012. “Adsorption/Desorption of Cd(II), Cu(II) and Pb(II) Using Chemically Modified Orange Peel: Equilibrium and Kinetic Studies.” *Solid State Sciences* 14 (2). Elsevier Masson SAS: 202–10. doi:http://dx.doi.org/10.1016/j.solidstatesciences.2011.11.029.
27. Liu, Huan, Dongqi Yu, Tianbiao Sun, Hongyun Du, Wentao Jiang, Yaseen Muhammad, and Lei Huang. 2019. “Fabrication of Surface Alkalinized G-C3N4 and TiO2 Composite for the Synergistic Adsorption-Photocatalytic Degradation of Methylene Blue.” *Applied Surface Science* 473 (April). North-Holland: 855–63. doi:10.1016/J.APSUSC.2018.12.162.
28. Mockaitis, G., J. a D Rodrigues, E. Foresti, and M. Zaiat. 2012. “Toxic Effects of Cadmium (Cd2+) on Anaerobic Biomass: Kinetic and Metabolic

Implications." *Journal of Environmental Management* 106 (September). Elsevier Ltd: 75–84. doi:10.1016/j.jenvman.2012.03.056.
29. Mohamed, Latifa A., Chukwunonso O. Aniagor, Ghada M. Taha, A. Abou-Okeil, and A. Hashem. 2021. "Mechanistic Investigation of the Mass Transfer Stages Involved during the Adsorption of Aqueous Lead onto Scopulariopsis Brevicompactum Fungal Biomass." *Environmental Challenges* 5 (December). Elsevier B.V. doi:10.1016/j.envc.2021.100373.
30. Nong, Guangzai, Zongwen Zhou, and Shuangfei Wang. 2016. "Generation of Hydrogen, Lignin and Sodium Hydroxide from Pulping Black Liquor by Electrolysis." *Energies* 9 (1): 13. doi:10.3390/en9010013.
31. Oboh, I O, and E O Aluyor. 2009. "Luffa Cylindrica" 4 (August): 684–88.
32. Oboh, Innocent, Emmanuel Aluyor, and Thomas Audu. 2009. "Biosorption of Heavy Metal Ions from Aqueous Solutions Using a Biomaterial." *Leonardo Journal of Sciences*, no. 14: 58–65.
33. Okunola, O. J., A. Uzairu, G. I. Ndukwe, and S. G. Adewusi. 2008. "Assessment of Cadmium and Zinc in Roadside Surface Soils." *Research Journal of Environmental Sciences* 2 (4): 266–74.
34. Plazinski, Wojciech, Wladyslaw Rudzinski, and Anita Plazinska. 2009. "Theoretical Models of Sorption Kinetics Including a Surface Reaction Mechanism: A Review." *Advances in Colloid and Interface Science* 152 (1–2). Elsevier B.V.: 2–13. doi:http://dx.doi.org/10.1016/j.cis.2009.07.009.
35. Rodriguez Correa, Catalina, Thomas Otto, and Andrea Kruse. 2017. "Influence of the Biomass Components on the Pore Formation of Activated Carbon." *Biomass and Bioenergy* 97 (Supplement C): 53–64. doi:https://doi.org/10.1016/j.biombioe.2016.12.017.
36. Saeed, Asma, Muhammad Iqbal, Saeed Iqbal Zafar, and Saeed Iqbal. 2009. "Immobilization of Trichoderma Viride for Enhanced Methylene Blue Biosorption: Batch and Column Studies." *Journal of Hazardous Materials* 168 (1): 406–15. doi:http://dx.doi.org/10.1016/j.jhazmat.2009.02.058.
37. Sangi, Mohammad Reza, Ali Shahmoradi, Javad Zolgharnein, Gholam Hassan Azimi, and Morteza Ghorbandoost. 2008. "Removal and Recovery of Heavy Metals from Aqueous Solution Using Ulmus Carpinifolia and Fraxinus Excelsior Tree Leaves." *Journal of Hazardous Materials* 155 (3): 513–22. doi:http://dx.doi.org/10.1016/j.jhazmat.2007.11.110.
38. Saueprasearsit, P., M. Nuanjaraen, and M. Chinlapa. 2010. "Biosorption of Lead(Pb2+) by Luffa Cylindrica Fiber...Saueprasearsit et Al., 2010.Pdf."
39. Saw, S K, R Purwar, S Nandy, J Ghose, and G Sarkhel. 2013. "Fabrication, Characterisation Ad Evaluation of Luffa Cylindrica Fiber Reinforced Epoxy Composites." *Bioresources* 8 (4).
40. Saw, Sudhir Kumar, Raghwendra Purwar, Sourabh Nandy, Joyjeet Ghose, and Gautam Sarkhel. 2013. "Fabrication, Characterization, and Evaluation of Luffa Cylindrica Fiber Reinforced Epoxy Composites" 8: 4805–26.
41. Shaikh, T, and S A Agrawal. 2014a. "Qualitative and Quantitative Characterization of Textile Material by Fourier Transform Infra-Red." *International Journal of Innovative Research in Science, Engineering and Technology* 3 (1).
42. Shaikh, T, and Shaikh and Agrawal. 2014b. "Qualitative and Quantitative Characterization of Textile Material by Fourier Transform Infra-Red." *International Journal of Innovative Research in Science, Engineering and Technology* 3 (1): 8496–8502.
43. Suhas, V. K. Gupta, P. J M Carrott, Randhir Singh, Monika Chaudhary, and Sarita Kushwaha. 2016. "Cellulose: A Review as Natural, Modified and Activated Carbon Adsorbent." *Bioresource Technology*. doi:10.1016/j.biortech.2016.05.106.
44. Tang, Wang-Wang Wang, Guang-Ming Ming Zeng, Ji-Lai Lai Gong, Jie Liang, Piao Xu, Chang Zhang, and Bin-Bin Huang. 2014. "Impact of Humic/Fulvic Acid on the Removal of Heavy Metals from Aqueous Solutions Using Nanomaterials; A Review." *Science of the Total Environment* 468–469 (January). Elsevier B.V.: 1014–27. doi:10.1016/j.scitotenv.2013.09.044.
45. Tsibranska, I, and E Hristova. 2011. "Comparison of Different Kinetic Models for Adsorption of Heavy Metals onto Activated Carbon from Apricot Stones." *Bulgarian Chemical Communications* 43 (3): 370–77.
46. Vilar, Vítor J P, Cidália M S Botelho, José P S Pinheiro, Rute F. Domingos, and Rui a R Boaventura. 2009. "Copper Removal by Algal Biomass: Biosorbents Characterization and Equilibrium Modelling." *Journal of Hazardous Materials* 163 (2–3): 1113–22. doi:http://dx.doi.org/10.1016/j.jhazmat.2008.07.083.
47. Whittaker, D. 2000. "Interpreting Organic Spectra [Royal Society of Chemistry]."
48. Williams, D, and I. Fleming. 2008. "Spectroscopic Methods in Organic Chemistry."
49. Yang, Bo, Jiane Zuo, Xinyao Xinhua Tang, Fenglin Liu, Xin Yu, Xinyao Xinhua Tang, Hui Jiang, and Lili Gan. 2014. "Effective Ultrasound Electrochemical Degradation of Methylene Blue Wastewater Using a Nanocoated Electrode." *Ultrasonics Sonochemistry* 21 (4). Elsevier B.V.: 1310–17. doi:10.1016/j.ultsonch.2014.01.008.
50. Zdarta, Jakub, Lukasz Klapiszewski, Marcin Wysokowski, Norman Malgorzata, Agnieszka

Kolodzeiejczak-Radzimska, Dariusz Moszyinski, Hermann Ehrlich, Hieronim Maciejewski, Allison L. Stelling, and Teofil Jesionowski. 2015. “Chitin-Lignin Material as a Novel Matrix for Enzyme Immobilization.” *Marine Drugs* 13 (4): 2424–46. doi:10.3390/md13042424.